LBL-37720
UC-406

# Lawrence Berkeley Laboratory
UNIVERSITY OF CALIFORNIA

Presented at SCINT '95, Delft, The Netherlands,
August 28–September 1, 1995, and to be published
in the Proceedings

## Scintillators for Positron Emission Tomography

W.W. Moses and S.E. Derenzo

September 1995

# Donner Laboratory
## Biology & Medicine Division

REFERENCE COPY
Does Not
Circulate
Bldg. 50 Library.
LBL-37720
Copy 1

Prepared for the U.S. Department of Energy under Contract Number DE-AC03-76SF00098

## DISCLAIMER

This document was prepared as an account of work sponsored by the United States Government. While this document is believed to contain correct information, neither the United States Government nor any agency thereof, nor the Regents of the University of California, nor any of their employees, makes any warranty, express or implied, or assumes any legal responsibility for the accuracy, completeness, or usefulness of any information, apparatus, product, or process disclosed, or represents that its use would not infringe privately owned rights. Reference herein to any specific commercial product, process, or service by its trade name, trademark, manufacturer, or otherwise, does not necessarily constitute or imply its endorsement, recommendation, or favoring by the United States Government or any agency thereof, or the Regents of the University of California. The views and opinions of authors expressed herein do not necessarily state or reflect those of the United States Government or any agency thereof or the Regents of the University of California.

*Presented at SCINT '95, Delft, The Netherlands* *LBL-37720*

# SCINTILLATORS FOR POSITRON EMISSION TOMOGRAPHY†

William W. Moses and Stephen E. Derenzo, Lawrence Berkeley National Laboratory,
University of California, Berkeley, CA 94720

## ABSTRACT

Like most applications that utilize scintillators for gamma detection, Positron Emission Tomography (PET) desires materials with high light output, short decay time, and excellent stopping power that are also inexpensive, mechanically rugged, and chemically inert. Realizing that this "ultimate" scintillator may not exist, this paper evaluates the relative importance of these qualities and describes their impact on the imaging performance of PET.

The most important PET scintillator quality is the ability to absorb 511 keV photons in a small volume, which affects the spatial resolution of the camera. The dominant factor is a short attenuation length (≤1.5 cm is required), although a high photoelectric fraction is also important (>30% is desired). The next most important quality is a short decay time, which affects both the dead time and the coincidence timing resolution. Detection rates for single 511 keV photons can be extremely high, so decay times ≤500 ns are essential to avoid dead time losses. In addition, positron annihilations are identified by time coincidence so ≤5 ns fwhm coincidence pair timing resolution is required to identify events with narrow coincidence windows, reducing contamination due to accidental coincidences. Current trends in PET cameras are toward septaless, "fully-3D" cameras, which have significantly higher count rates than conventional 2-D cameras and so place higher demands on scintillator decay time. Light output affects energy resolution, and thus the ability of the camera to identify and reject events where the initial 511 keV photon has undergone Compton scatter in the patient. The scatter to true event fraction is much higher in fully–3D cameras than in 2-D cameras, so future PET cameras would benefit from scintillators with a 511 keV energy resolution <10–12% fwhm.

## OVERVIEW OF PET CAMERA DESIGN

The PET camera detects coincident pairs of 511 keV annihilation photons with a circular array of detector modules that encircles the patient as shown in Figure 1, with each detector module

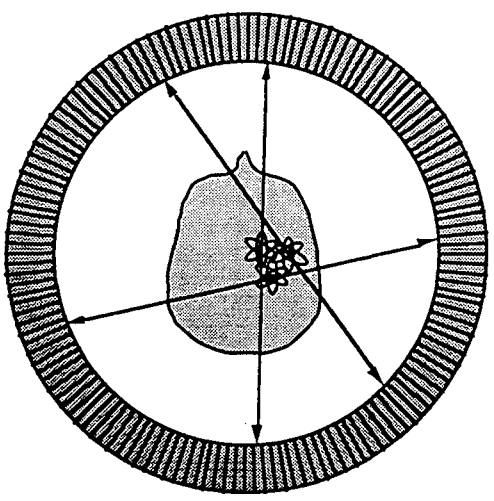

**Fig. 1: PET Camera.**
The patient is injected with a drug containing a positron emitting isotope, which localizes in a biologically active area in the patient. The isotope decays, and annihilates with an electron from the tissue to form back to back 511 keV photons. These penetrate the patient and are detected via time coincidence in a detector ring that encircles the patient. The decay was then known to occur somewhere on the line connecting the two detector elements, also known as a chord. Using the coincidence rates measured in each chord, the mathematical technique of computed tomography forms a two dimensional image of the isotope distribution (and hence drug distribution) in the plane defined by the tomograph ring.

†This work was supported in part by the Director, Office of Energy Research, Office of Health and Environmental Research, Medical Applications and Biophysical Research Division of the U.S. Department of Energy under contract No. DE-AC03-76SF00098, and in part by Public Health Service Grant No. R01 CA48002 awarded by the National Cancer Institutes, Department of Health and Human Services.

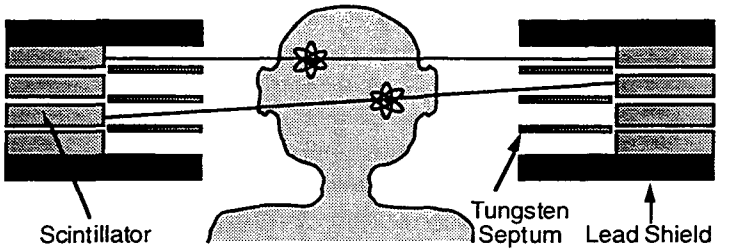


**Fig. 2: Multi-Ring Camera.** Several rings can be stacked and data simultaneously accumulated to form a 3 dimensional image. Removable tungsten septa reduce Compton scatter from the patient, but decrease the efficiency by limiting the number of cross-plane slices allowed.

potentially in coincidence with each of the detector modules on the opposite side of the ring. Such a ring can then images a two dimensional slice of the activity in that detector plane. Most modern PET cameras contain several stacked detector planes, as shown in Figure 2. This allows several slices (including cross-plane slices, in which the 511 keV photons are detected in different detector rings) to be acquired simultaneously, and the resulting planar images stacked to form a three dimensional image. Interplane tungsten septa collimate the annihilation photons, reducing background from Compton scatter in the patient but limiting the detection efficiency for the cross-plane slices and so the overall detection efficiency. In Fully 3-D PET these septa are often removable so that data from all cross-plane slices can be acquired [1].

## PET DETECTOR REQUIREMENTS

The requirements for an individual PET detector module have been described previously [2]. It must identify the 511 keV photons with: (1) high detection efficiency (>85% per 511 keV photon), (2) high spatial resolution (<5 mm fwhm), (3) low cost (parts cost <$600 / in$^2$ of "front" surface area), (4) low dead time (<4 μs in$^2$,where the figure of merit is the product of the detector dead time and the front surface area of the portion of the detector that is dead), (5) good timing resolution (<5 ns fwhm), and (6) good energy resolution (<100 keV fwhm). These requirements are listed in approximate order of decreasing importance.

The first PET detector modules consisted of a single scintillator crystal coupled to a photomultiplier tube (PMT), as shown in Figure 3a. The width and height of the crystal determine the in-plane and axial resolution respectively, while the depth (typically 3 attenuation lengths) determines the detection efficiency. This design has excellent performance, but is expensive (due to the large number of PMTs needed), does not allow small scintillator crystals to be used (due to the minimum size of PMTs), and is difficult to form the crystals into a close-packed two-dimensional array. Therefore, current PET cameras generally use detector modules similar to that shown in Figure 3b [3]. The 511 keV photons interact in the BGO scintillator

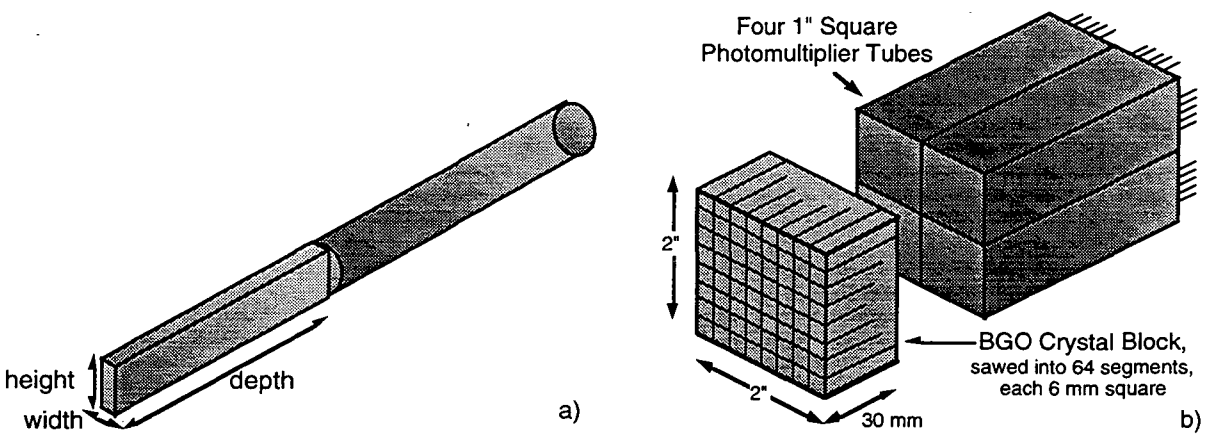


**Fig. 3a): Early PET Detector Module.** The earliest PET detector modules consisted of a PMT coupled to a single scintillator crystal (at first NaI:Tl, then BGO after its discovery). **3b): Modern PET Detector Module.** Four photomultiplier tubes decode which of the 6x6x30 mm crystal segments the 511 keV photon interacts in. The scintillation light is distributed across the back face of the BGO crystal, where Anger logic (*i.e.* the ratio of the four PMT output signals) determines the segment of interaction.

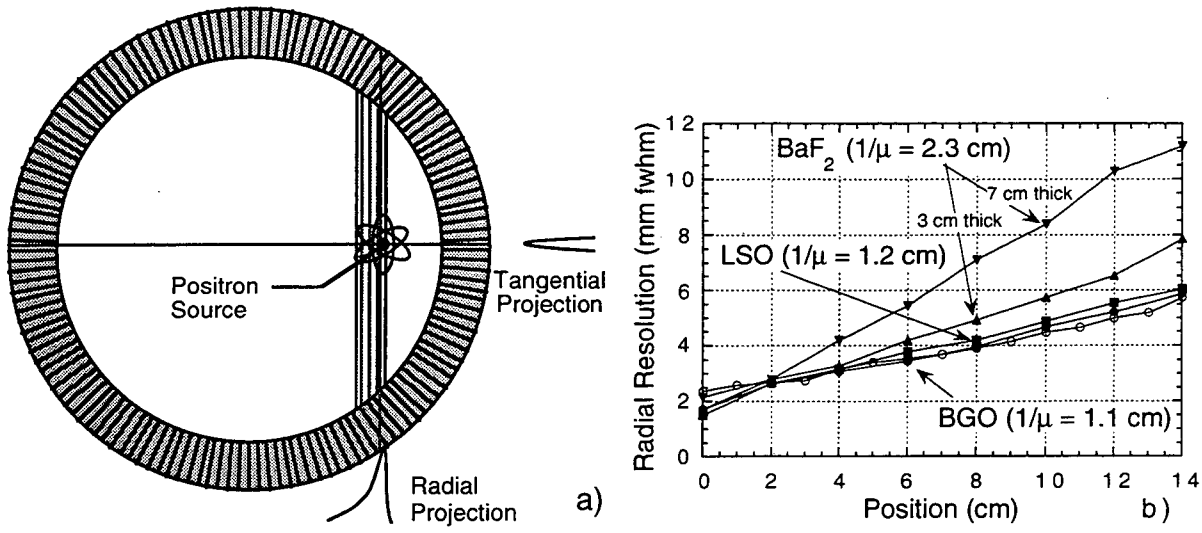


**Fig. 4a): Cause of Radial Elongation.** 511 keV photons that are incident at an oblique angle can penetrate into the detector ring before interacting and being detected. This causes a blurring that worsens as the source is moved away from the center of the ring. **4b): Effect of Attenuation Length on Radial Elongation.** Monte Carlo simulation of the reconstructed resolution as a function of position for 3 cm deep tomographs made of various scintillators. The closed circles are BGO, the squares are LSO, the triangles $BaF_2$, and the open circles measured data with a BGO tomograph. The inverted triangles are for a tomograph constructed of 7 cm deep $BaF_2$ scintillator.

crystal, and the resulting scintillation light observed by four PMTs. BGO [4] is commonly used, as its attenuation length (1.1 cm) is lower than any other commonly available scintillator. The 30 mm depth of the BGO crystal is nearly 3 attenuation lengths, ensuring high detection efficiency. Saw cuts in the BGO define "individual" crystal elements by controlling the light distribution among the four PMTs, and Anger logic (*i.e.* analog ratios among the four PMT signals) is used to determine which of the "individual" crystals the interaction occurred in. The sum of the four PMT signals is used to form a timing pulse (with 3 ns fwhm accuracy) and a measurement of the photon energy (with 100 keV accuracy). The size of the "individual" crystal elements determines the position resolution of the detector module, but a limited number of crystals (typically ≤64) can be accurately decoded due to the limited light output of BGO. The entire module is "dead" for approximately 1 μs after a 511 keV photon interaction while the BGO emits its scintillation light (its decay time is 300 ns), as interaction in any other portion of the module during this time would confuse the Anger logic.

## SCINTILLATOR REQUIREMENTS FOR PET

The scintillator requirements for PET are best determined by evaluating their affect on the PET detector requirements listed in the previous section. Using the BGO as a standard, the requirements for a scintillator for PET (all quantities assume 511 keV photon energy), listed in approximate order of decreasing importance, are as follows: (1) short attenuation length (<1.5 cm), (2) high photoelectric fraction (>30%), (3) short scintillation decay time (<500 ns), (5) low cost (<$20/cc), and (6) high light output (>8000 photons/MeV). The remainder of this paper discusses the basis for these requirements in more detail.

### Attenuation Length

With any PET detector design, a high detection efficiency (>85%) is necessary, which implies that the detector depth (*i.e.* thickness in the radial direction) be at least two attenuation lengths thick, and preferably three. While this criterion can be met with a scintillator of any attenuation length, a short attenuation length is desired to minimize a resolution degradation artifact caused by penetration of the 511 keV photons into the crystal ring. The origin of this

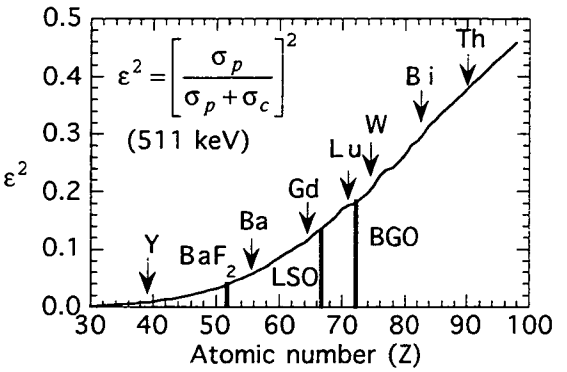


**Fig. 5: Double Photoelectric Interaction Probability.**
The probability that both annihilation photons interact via the photoelectric effect as a function of effective atomic number. Note the strong increase with increasing atomic number.

artifact, variously known as radial elongation, parallax error, or radial astigmatism, is shown in Figure 4a. Photons that are normally incident on the detector ring are detected in the crystal that they impinge upon no matter how far they penetrate into the ring before interacting. However, photons that impinge on the detector ring at an oblique angle can penetrate into adjacent crystals before they interact and are detected, which causes mis-positioning errors (*i.e.* events are assigned to chords that do not pass through the source). This spatial resolution degradation increases for objects placed further away from the center of the tomograph ring.

Figure 4b shows the magnitude of this effect for various different scintillator materials. It plots the full width at half maximum (fwhm) of the reconstructed image of a point source as a function of the distance of that point source from the center of the tomograph ring. Data were created with a Monte Carlo simulation of a 60 cm diameter tomograph ring made up of 3x3x30 $mm^3$ crystals of various scintillators, and validated with a BGO tomograph with the same dimensions (the open circles in Figure 4b). The data show that the resolution is worse at large distances from the center even for BGO (1.2 cm attenuation length), but that the degradation in LSO [5] (1.3 cm attenuation length) is similar to that of BGO. It also shows that a 3 cm thick ring of $BaF_2$ (2.3 cm attenuation length) has considerably poorer resolution and a significantly reduced detection efficiency. If the $BaF_2$ thickness is increased to 7 cm (to have a similar number of attenuation lengths as the BGO or LSO tomographs), the degradation becomes severe. This is the main reason that virtually all PET cameras use BGO scintillator.

## Photoelectric Fraction

Photoelectric interactions are greatly preferred over Compton scatter, as 511 keV photon interactions that Compton scatter deposit energy in two (or more) locations in the detector ring, frequently separated by >1 cm, and thus reduces the spatial resolution of the detector module. Figure 5 plots the probability that both 511 keV photons interact via a photoelectric interaction as a function of the atomic number. This probability increases rapidly with increasing atomic number, so scintillators containing a large fraction of high Z materials are desired. It is difficult to quantitate the magnitude of this effect, but the similarity of the resolution curves in Figure 4b for BGO (18.5% double photoelectric probability) and LSO (11.6% double photoelectric probability) indicate that the resolution is more sensitive to the attenuation length.

## Decay Lifetime

The decay lifetime affects both the timing resolution and the dead time. Assuming that multiple decay lifetime components are present, the dead time is influenced most by the slowest decay component. While the relationship between the decay time and the dead time is difficult to quantitate (especially with multiple decay lifetimes), most PET cameras trigger at the single photoelectron level, so the dead time can be defined as the time that it takes for the scintillation intensity to drop to the level of 1 photon/MeV/ns.

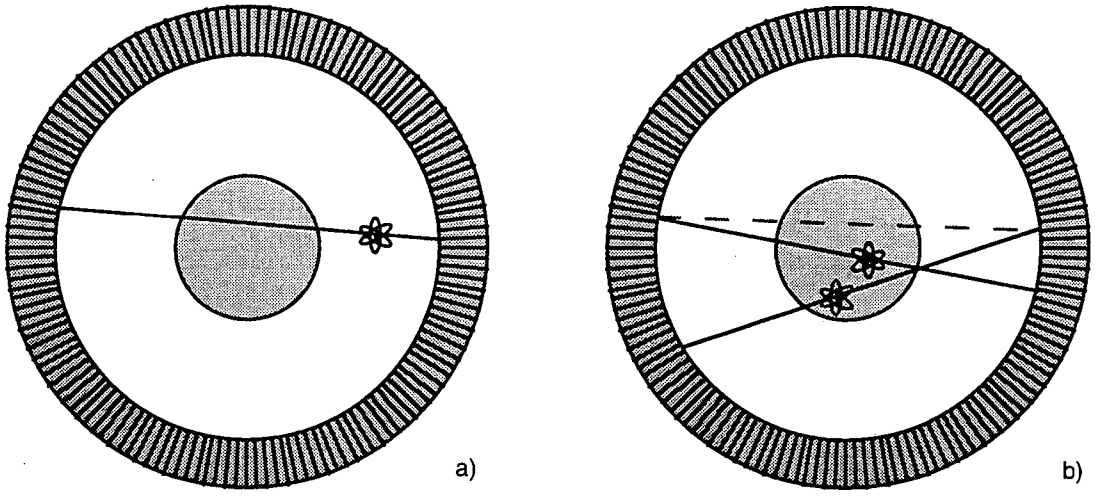


**Fig. 6a): Transmission Scans.** The attenuation within the patient is measured with an orbiting external source. The correction factor is given by the ratio of count rates with and without the patient in the scanner. **6b): Random Coincidences.** Simultaneous decays can cause random coincident events (dashed line).

Low dead time is critical as it affects the portion of a PET study known as the transmission scan. This is a scan that is used to correct for the 511 keV photon attenuation within the patient. It is performed with an orbiting external positron source, as shown in Figure 6a — the ratio of the count rate with the patient in the tomograph ring and with no patient gives the attenuation factor on a chord by chord basis. The strength of the external source is presently limited by the count rate in the detector modules closest to the source, which approaches 1 Mhz/in$^2$. Higher source strengths (1 to 2 orders of magnitude) are desired to decrease the time it takes to perform a transmission scan.

Timing resolution is determined by $I_0$, the scintillation photon intensity (photons/MeV/ns) immediately after excitation [6]. Again assuming that a scintillator has multiple decay lifetime components, the fastest component usually has the largest affect on $I_0$. Good timing resolution (<5 ns fwhm) is necessary in order to reduce random coincidences, as shown in Figure 6b. The random coincidence rate is given by $2S^2\Delta t$, where S is the singles rate and $\Delta t$ is the coincidence window width (typically 10 ns). Randoms become increasingly important when imaging higher activities (such as when imaging with short half-life isotopes) or with fully 3-D PET (which has a much higher efficiency than conventional PET, and random fractions can exceed 50%), as the coincidence rate scales linearly with the activity being imaged (*i.e.* like S) while the randoms rate scales like $S^2$. Better timing resolution will allow shorter coincidence windows to be used to reduce the random fraction. However, the minimum coincidence width is 4 ns, due to time of flight differences across the tomograph ring.

If the timing resolution is good enough, this decay time difference can be used to localize the position of the annihilation along chord [7]. Tomographs using $BaF_2$ scintillator have been built using this principle, but are not common. The system-wide coincidence timing resolution is typically 500 ps fwhm (it is difficult to keep the large number of crystals in a PET camera in mutual calibration), which localizes the annihilation to a line segment approximately 8 cm long. While this is considerably greater than the size of the scintillator crystal, the added information can be used by the reconstruction algorithm to reduce noise in the image.

## Luminosity

The luminosity affects the timing, spatial, and energy resolution. The affect on timing is simple — for a given decay time, a higher luminosity yields a higher initial intensity $I_0$ and so better timing resolution, as discussed previously. The effect on the spatial resolution lies in the ability of the block detector module to decode the crystal of interaction, which is limited by counting statistics. With a more luminous scintillator, more crystals can be decoded with the same

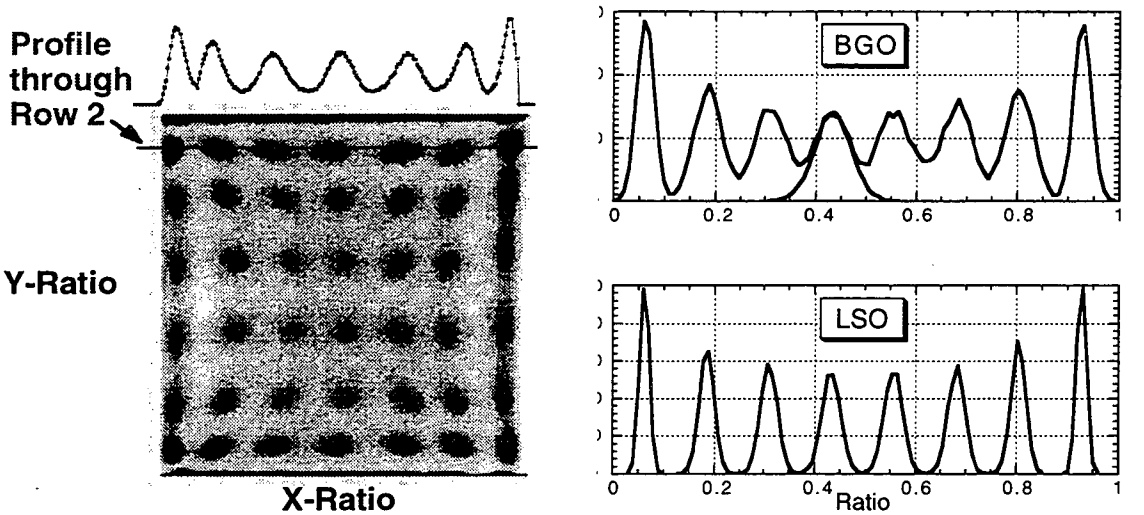


**Fig. 7a): Decoding in the Block Detector.** The block detector is uniformly illuminated with 511 keV photons, and for each interaction the X and Y position estimators are computed, then plotted as a point on the scatter plot at the left. Distinct dark regions are observed corresponding to crystal positions. A profile drawn through one row shows that there is some overlap between individual crystals. **7b): Dependence on Light Output.** Using a Monte Carlo simulation whose only blurring factor is statistical fluctuations, the overlap between crystals with the same luminosity as BGO is comparable to the experimentally measured overlap, while the overlap between crystals with the same luminosity as LSO is significantly smaller.

number of PMTs, allowing the crystal size to become smaller and thus achieve higher resolution. Present BGO based detector modules generate <200 photoelectrons per 511 keV interaction and decode up to an 8x8 array. Figure 7a plots the distribution of the X position estimator (*i.e.* the PMT ratio along one axis) when a 7x8 detector module is uniformly illuminated with 511 keV photons [8]. Seven peaks corresponding to the 7 crystals in this dimension are clearly seen, but there is some overlap and so some crystal mis-identification is present. Figure 7b shows similar distributions acquired from Monte Carlo simulations of an 8x8 array with light outputs equal to that of BGO and LSO, where the only blurring effect is the counting statistics. The peaks overlap significantly when a light output equal to that of BGO is used, but have almost no overlap when the light output of LSO is used.

Higher luminosity can also help reduce background due to Compton scatter in the patient by improving the energy resolution. As the annihilation photons lose energy when they scatter, good energy resolution (for which high light output is necessary) will allow these scattered events to be identified and rejected. With BGO based block detectors, the 511 keV energy resolution is 12%–20% fwhm and a lower energy threshold is typically set at 350 keV. With these parameters, conventional 2-D PET (*i.e.* with septa) has approximately 15% of the coincidences contain scattered photons, while the fraction approaches 50% with fully 3-D PET.

## Emission Spectrum

The only requirement on the emission spectrum is that it be a good match to inexpensive PMTs. As this implies PMTs with bialkali photocathodes and borosilicate glass windows, this implies emissions in the range of 300–500 nm.

## Materials Considerations

Given that short attenuation length and high effective atomic number are mandatory, the major materials consideration is cost! A commercial tomograph uses approximately 8 liters of scintillator crystal and 500 PMTs. The parts cost of the scintillator and PMTs are each about

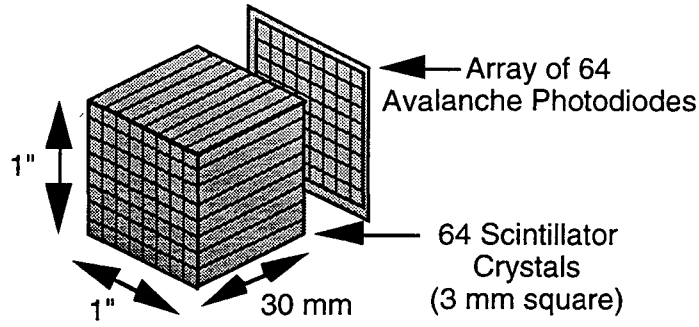


**Fig. 8: Solid State Photodetector PET Detector Module.**
The module consists of 64 optically isolated scintillator crystals, each 3 mm x 3 mm x 30 mm deep. When a 511 keV photon interacts in any of the elements, the scintillation light is detected by one element of an APD array located at one end of the crystal.

25% of the total parts cost, and the next most expensive item is approximately 5% of the total parts cost. Thus, any change compared to the cost of BGO (roughly $20/cc) will have a significant impact on the overall cost of the system.

It is also mandatory that the scintillator have good mechanical ruggedness in order to withstand the multiple saw cuts necessary to make the detector. This is one of the major reasons that GSO [9] is not found in modern tomographs. Many of the other materials properties can be compromised — radiation hardness and afterglow are not issues, and hygroscopic crystals can be used (NaI:Tl and CsF have been used reasonably often).

## FUTURE DIRECTIONS

### Fully 3-D PET

One of the major present directions that significantly affects the scintillator is fully 3-D PET. As mentioned earlier, it places more severe demands on the dead time and energy resolution than conventional 2-D PET. Presently, BGO is the dominant scintillator for 3-D PET, largely because most 3-D scanners are combination 2-D / 3-D scanners (*i.e.* have removable septa) and because no reasonable alternative exists. The majority of the scans performed in a clinical environment are 2-D, as 3-D scans are hampered by relatively poor detector performance and a much larger data set size.

### Time of Flight PET

Time of flight PET has long been a desired goal, but has not realized its potential due to scintillator deficiencies. A number of time of flight scanners have been made with $BaF_2$, but the extreme UV color of the fast light is difficult to work with, and the poor attenuation length and effective atomic number have compromised its spatial resolution or efficiency. A few scanners have also been made with CsF, which has similar problems with poor attenuation length and effective atomic number. Should a scintillator be discovered that combines the high initial luminosity of $BaF_2$ with short attenuation length, PET would be improved significantly.

### Solid State Photodetectors

One of the most exciting potential developments is the replacement of the PMT with a solid state photodetector such as an avalanche photodiode (APD) array, as shown in Figure 8. The successful development of economical, reliable APD arrays would significantly alter the requirements for PET scintillators. First, the lower signal to noise ratio in these devices (compared to a PMT) would require higher luminosity and initial intensity in order to achieve the requisite timing and energy resolution. The fact that each scintillator crystal is an independent detector element greatly reduces the dead time, and so decay lifetimes up to approximately 10 μs can be tolerated. The quantum efficiency of APDs is significantly higher

than PMTs, so the limits put on energy resolution by counting statistics are reduced and better energy resolution may be achievable. Finally, silicon based photodetectors have good quantum efficiency in a different wavelength range than PMTs (400–900 nm rather than 300–500 nm), so it is possible to use scintillators that emit at much longer wavelengths.

## CONCLUSION

The most important scintillator property for PET is good stopping power, loosely defined as the combination of short attenuation length and high effective atomic number. The next most important attributes, in order of decreasing importance, are decay lifetime, light output, and cost. Greatly improved PET scanners would result if scintillator materials were developed that had similar characteristics to BGO, but with better energy resolution or shorter decay lifetime. Finally, solid state photodetectors would allow a significantly different set of compromises to be made, but also have tremendous potential for improving PET.

## ACKNOWLEDGMENTS

We thank our colleagues working in radiation detection and medical imaging research for the innumerable thought provoking discussions that have lead to this summary. This work was supported in part by the Director, Office of Energy Research, Office of Health and Environmental Research, Medical Applications and Biophysical Research Division of the U.S. Department of Energy under contract No. DE-AC03-76SF00098, and in part by Public Health Service Grant Nos. P01 HL25840, R01 CA48002, and R01 NS29655, awarded by the National Heart Lung and Blood, National Cancer, and Neurological Science Institutes, Department of Health and Human Services.

## REFERENCES

[1] Cherry SR, Dahlbom M and Hoffman EJ. 3D PET using a conventional multislice tomograph without septa. *J. Comput. Assist. Tomogr.* **15:** pp. 655–668, 1991.

[2] Moses WW, Derenzo SE and Budinger TF. PET detector modules based on novel detector technologies. *Nucl. Instr. Meth.* **A-353:** pp. 189–194, 1994.

[3] Tornai MP, Germano G and Hoffman EJ. Positioning and energy response of PET block detectors with different light sharing schemes. *IEEE Trans. Nucl. Sci.* **NS-41:** pp. 1458–1463, 1994.

[4] Weber MJ and Monchamp RR. Luminescence of $Bi_4Ge_3O_{12}$: spectral and decay properties. *J Appl Phys* **44:** pp. 5495-5499, 1973.

[5] Melcher CL and Schweitzer JS. Cerium-doped lutetium orthosilicate: a fast, efficient new scintillator. *IEEE Trans. Nucl. Sci.* **NS-39:** pp. 502–505, 1992.

[6] Hyman LG. Time resolution of photomultiplier systems. *Rev. Sci. Instr.* **36:** pp. 193–196, 1965.

[7] Ter-Pogossian MM, Mullani NA, Ficke DC, et al. Photon time-of-flight-assisted positron emission tomography. *J Comput Assist Tomogr* **5:** pp. 227-239, 1981.

[8] Cherry SR, Tornai MP, Levin CS, et al. A comparison of PET detector modules employing rectangular and round photomultiplier tubes. *IEEE Trans. Nucl. Sci.* **NS-42:** pp. 1064–1068, 1995.

[9] Takagi K and Fukazawa T. Cerium-activated $Gd_2SiO_5$ single crystal scintillator. *Appl. Phys. Lett.* **42:** pp. 43–45, 1983.

LAWRENCE BERKELEY LABORATORY
UNIVERSITY OF CALIFORNIA
TECHNICAL INFORMATION DEPARTMENT
BERKELEY, CALIFORNIA 94720